Groundwater Necrophagy: The Role of Dead Microbes on the Subsurface Microbiome

Mariam Alsaid

ABSTRACT

Much of the earth's carbon is stored underground due to microbes' significant role in carbon cycling. Recent studies have suggested that necromass (ie. non-living microbial biomass) may constitute a large portion of the subsurface carbon pool. This raises the question of how living subsurface microbes interact with necromass and whether they are a driving force in its turnover. The goal of this project is to investigate the dynamics of necromass consumption in groundwater microbial communities. In order to get an in-depth understanding of this phenomenon, I asked three main questions: 1) Does the chemical composition of artificial necromass differ depending on the cell lysate used to produce it? 2) Does variability in necromass composition influence microbial communities over time? 3) Which necromass-consuming microbes can be isolated from groundwater enrichments in artificial necromass? To investigate these questions, I produced artificial necromass derived from 5 subsurface bacterial strains and utilized it as a substrate to promote the growth of subsurface groundwater microbes. I then enriched groundwater microbial communities in this artificial necromass and observed as their community compositions varied in response to the type of necromass provided. Lastly, I isolated 17 distinct bacterial strains from these enrichment cultures. Results from this study indicate that necromass plays a significant role in shaping microbial communities and will help us in understanding how carbon is utilized in the subsurface environment.

KEYWORDS

Soil ecology, microbiology, subsurface, necromass, carbon cycle

INTRODUCTION

Soil organic matter (SOM) refers to the carbon pool resulting from the gradual deposition of plant carbon inputs and functions as a massive carbon sink, accumulating two times more carbon than what is stored in the atmosphere and three times more than in vegetation (Eswaran et al. 1993). The majority of research on SOM's role in global carbon cycling focuses on surface soils and related plant-microbial interactions. However, subsurface carbon-mineral associations and microbial communities have been observed to significantly influence soil organic matter dynamics (Jackson et al. 2017). A paradigm shift in the field of soil ecology has revealed that SOM is majorly composed of microbial matter as opposed to plant litter or debris, suggesting that microbial communities directly shape the nature and abundance of SOM (Liang et al. 2019). Anabolic metabolic activity by subsurface microbes directly affects SOM through the transformation of inorganic ions into cellular components or metabolites (Basile-Doelsch et al. 2020). From an environmental perspective, microbial ecology research promotes the idea that soil and its associated microbiota is a valuable resource in combating the harmful levels of carbon dioxide emissions (Buckeridge et al. 2022). Researching the role that microbial communities play in their respective ecosystems may help us to gain insight into the factors that influence carbon turnover rates, giving us a better understanding of carbon cycling dynamics as a whole.

In addition to carbon cycling, SOM facilitates the transport of nutrients in soil, namely nitrogen and phosphorus (Kastner et al. 2021). This is attributed to the fact that necromass (ie. non-living microbial biomass) constitutes 15-80% of SOM, which enables carbon and nutrient cycling during its turnover. Necromass typically consists of polysaccharides, proteins, enzymes, and DNA that were exuded from the cytoplasm, biofilm, or hyphal mucilage of intact or burst microbiota (Buckeridge et al. 2022). Researching the microorganisms that consume this material will be beneficial in our understanding of the carbon cycle and determining the extent that soil behaves as a carbon sink (Dong et al. 2021, Sokol et al. 2018). A recent study found that enriching soil in complex carbon sources such as necromass in the form of cell lysate and sediment dissolved organic matter (DOM) yielded more diverse microbial communities when compared to enrichments done in simple carbons such as glucose, acetate, benzoate, oleic acid, cellulose, and vitamins (Wu et al. 2020). This further emphasizes the need for diversifying our approaches regarding microbial enrichments in order to get a better idea of how microbes behave

in their natural and incredibly complex environments.

Necromass decomposition is facilitated by microbial metabolism and mechanical disruption of soil. Given that microbially derived necromass is an important component of SOM, and that microbial metabolism directly plays an essential role in its turnover, necromass consumption is likely a common mechanism in these ecosystems (Buckeridge et al. 2022). The consumption of necromass by predatory or scavenging microbial species can occur through the secretion of enzymes or other prey-specific antimicrobial metabolites and proteins that lyse cells externally (Martins et al. 2022). Additionally, some species have been observed to invade the periplasm of their prey, resealing it, and consuming the cell's contents (Martins et al. 2022). Mechanical disruption of soil through bioturbation by macrofauna helps to increase the contact between different carbon sources and the organisms that utilize them (Basile-Doelsch et al. 2020). Regardless of how frequently bioturbation occurs, necromass decomposition rates are ultimately dependent on microbial metabolic activity (Kastner et al. 2021). Determining which microbes utilize necromass as an energy source will allow us to get a better understanding of global carbon dynamics in soils.

The full impact of soil microbiota's carbon use efficiency, or the ability to convert absorbed carbon into biomass carbon, is not yet fully understood (Adingo et al. 2021). By learning more about the subsurface microbiome's role in the carbon cycle, we can better understand the underlying interactions that promote carbon sequestration abilities. This will subsequently allow us to mitigate the magnitude of carbon that is released into the environment, contributing to climate change (Bradford et al. 2016, Sokol et al. 2018). With the knowledge that necromass is a main component of SOM, my study aims to understand the dynamics of groundwater microbial necrophagy. To aid me in my research, I optimized a protocol to produce artificial necromass derived from several bacterial strains. I then conducted a metabolomics analysis on these samples to determine whether the chemical composition of necromass varies across different strains of bacteria. Next, I enriched a groundwater sample in these different strains of necromass and observed how the microbial community composition changed over time in these different treatment conditions. Lastly, microbes enriched in my experimentation were also isolated using this artificial necromass as a carbon source for future studies on necrophagy dynamics. I hypothesized that necromass chemical composition does vary depending on the species of cell lysate utilized. I also expected the introduction of necromass to greatly influence the resulting microbial community composition, and for this impact to also be shaped by the variety of

necromass utilized.

METHODS

Sample Collection

Groundwater samples were collected from the Oak Ridge Reservation Field Research Center (ORR FRC) at Y12 National Security Complex in Tennessee, USA (Watson et al. 2004). Groundwater samples were collected from the mid-screen level using a peristaltic pump at low flow to minimize drawdown into the well. After approximately 2 to 20 liters of groundwater was purged from each well, these samples were stored at 4 °C. To prepare samples for incubation with artificial necromass, around 50 mL of the collected groundwater was spun down at 6,500 g for 8 minutes using a floor centrifuge to get a high starting cell density.

Artificial Necromass Production

To create artificial necromass, I chose five isolates that were commonly isolated from ORR FRC (Table 1). Because of their abundance in this site, these strains are likely contributors to the necromass pool at this site, therefore making them good candidates for our study. These five isolates were revived from glycerol stocks and streaked onto R2A agar plates and incubated at 30°C for a period of 3-5 days. Once visible colonies grew, I inoculated a colony from each plate into 1 mL of liquid basal media (0.25g/L NH_4Cl, 0.60 g/L NaH_2PO_4, 0.10 g/L KCl, 2.50 g/L $NaHCO_3$, 10 mL/L each of DL vitamins and DL minerals, 1.8 g/L D-glucose) and stored them in a shaking incubator at 30°C. This media acts as a minimal media that is less likely to be used as a carbon source in my enrichment experiment. Once the 1 mL cultures became turbid, I scaled them up to 10 mL by inoculating this volume in 9 mL of the basal media. After these 10 mL cultures became turbid, I measured and recorded the optical densities (OD) at 600 nm using a Biotek Epoch 2 Plate Reader. If the OD was greater than 0.3, I scaled these cultures up to 100 mL by inoculating them in 90 mL of the basal media. After incubating these 100 mL cultures for several days, I monitored their growth until their OD measurement was around 0.4, at which point I began harvesting their pellets.

I split each 100 mL culture into four 25 mL aliquots and spun these samples down at 6,000 g for 15 minutes in a Beckman floor centrifuge. Centrifuging liquid cultures pellets the biomass

generated and removes the basal medium supernatant, preventing nutrients from residual media to be included in the artificial necromass. I pipetted out and discarded the supernatants and stored the pellets at -80°C until lysis. To aid in dislodging the pellets during lysis, I pipetted 1 mL of 30 mM sodium bicarbonate buffer into each tube, combined these samples into one tube, and vortexed the solution. I then pipetted 1 mL of the homogenized solution into four 1.5 mL eppendorf tubes and sonicated using a probe sonicator at 40 power for five rounds of 30 seconds each, making sure to sterilize the probe with ethanol between rounds. Next, I filter-sterilized the lysate using a 0.22 nm filter so that any intact/surviving cells were removed from my samples.

Total Organic Carbon Measurements and Metabolomics Analysis

I measured the total organic carbon of each lysate using a TOC Analyzer. This instrument heats samples to very high temperatures and calculates the concentration of carbon in parts per million (ppm) by quantifying the amount of CO_2 generated during combustion. Measuring the amount of carbon in my artificial necromass samples is necessary to ensure that I introduce equal concentrations of carbon in each of my treatment groups. Samples from these lysates were then run through an Liquid Chromatograph-Mass Spectrometer (LC-MS). Through a targeted metabolomics approach, the LC-MS estimated the relative abundances of specific chemical compounds in each of my five individual necromass samples, in addition to a mixed necromass sample. Metabolite composition was analyzed and visualized in R using the following packages: *factoextra, pheatmap, cluster, ggplot2,* and *tidyverse* (Kassambara and Mundt, 2020; Kolde, 2012; Maechler et al. 2022; Wickam, 2016; Wickam et al. 2019)

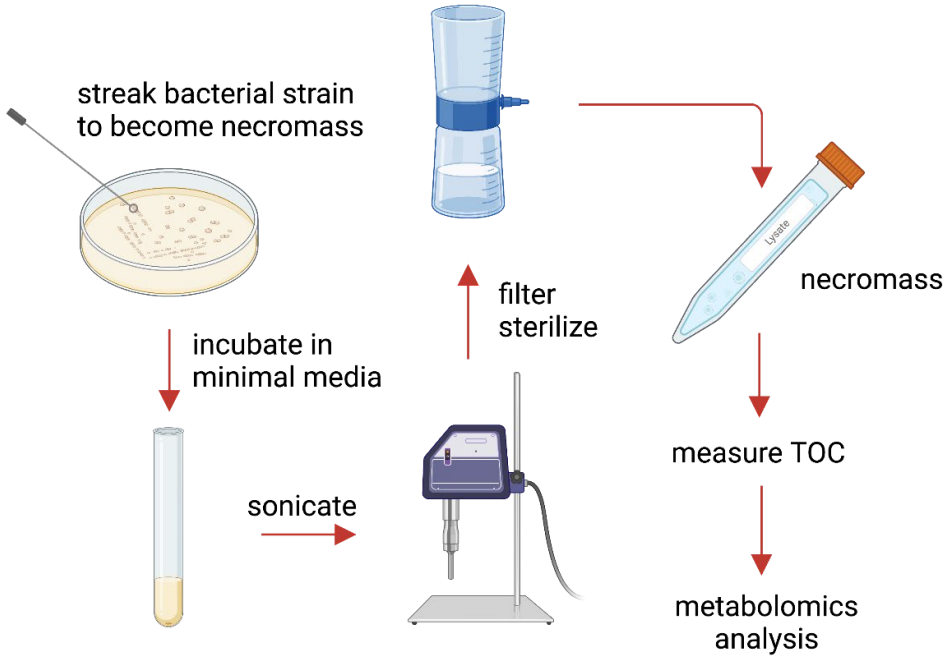

Figure 1. An optimized protocol for the generation of artificial necromass. This protocol consisted of streaking isolates onto R2A plates, incubating them in basal media, sonicating them with a probe sonicator, filter sterilizing them, measuring their total organic carbon, and analyzing their metabolites.

Groundwater Enrichments in Necromass

Groundwater enrichments were conducted in a total of seven different conditions: 5 individual necromass strains, 1 mixed necromass treatment, and 1 control condition consisting of only groundwater and basal media. 30 mL sealed serum bottles were used for this experiment. Each bottle contained 14 mL of liquid culture: 1.4 mL groundwater, X mL 30 ppm necromass, and the remaining volume consisted of our basal media. This experiment was performed in triplicate for a total of 21 cultures. These cultures were incubated for a period of 3 weeks and were sampled every 7 days. At each sampling interval, I punctured the stopper of each serum bottle with a hypodermic needle and collected 1 mL of culture for 16S amplicon sequencing; these samples were pelleted and stored at -20 °C. Glycerol stocks from each culture were also made at each timepoint by combining 1 mL of culture with 0.5 mL 50:50 basal media and glycerol. Glycerol stocks were stored at -80 °C.

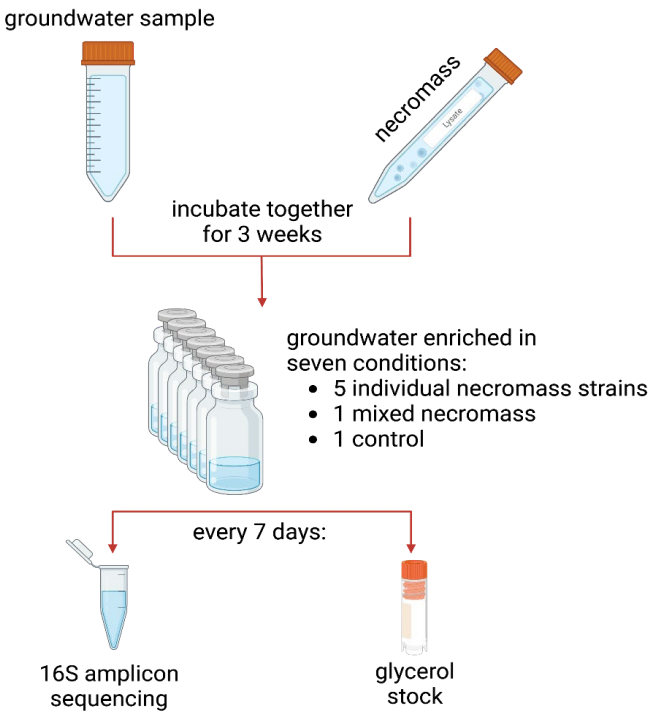

Figure 2. Experimental design for groundwater enrichments in necromass. This experiment was conducted in triplicates.

Pellets from my enrichment experiment were extracted using the Qiagen Powersoil Powerlyzer Kit. These samples were then sent to Novogene Co. for 16S DNA amplicon sequencing. I analyzed the 16S data using the microbial bioinformatics platform, Quantitative Insights Into Microbial Ecology 2 (QIIME2), which allowed me to visualize the microbial communities that were actively consuming our artificial necromass over time (Boylen et al. 2019). Alpha and beta diversity analysis was also performed in R using the packages *DESeq2, phyloseq*, *vegan,* and *tidyverse* (Love et al. 2014; McMurdie and Holmes, 2014; Oksanen et al. 2020; Wickam et al. 2019).

Isolation Efforts from Groundwater Enrichments in Necromass

The glycerol stocks from my last timepoint were revived on basal media agar plates by spreading 50 uL of 30 ppm necromass followed by 100 uL of the groundwater enrichment stock on the plate. Groundwater was spread onto plates in 3 different dilutions: undiluted, 10^{-1}, and 10^{-2}. Once colonies started to form, distinct morphologies were picked and restreaked onto fresh basal media + necromass plates. If this transfer looked pure, I inoculated a colony in 5 mL of liquid

R2A media and monitored its growth. Once cultures were turbid, I looked at them under the microscope and made note of their morphologies. These cultures were then made into glycerol stocks and pelleted to be sent to the UC Berkeley Sequencing Facility for DNA extraction. I conducted PCR on these isolates using full length 16S primers and sent them for Sanger sequencing at the UC Berkeley Sequencing Facility. Lastly, I analyzed sequences using the bioinformatic software, Geneious Prime 2023.1.2.

RESULTS

Necromass Composition

The cluster map shown in Figure 3 was constructed by running each of my individual artificial necromass strains (Table 1), as well as a mixed necromass trial, through an LC-MS instrument. A targeted metabolomics approach was conducted by qualitatively measuring the relative abundance of 47 commonly found intracellular metabolites. These 47 metabolites, consisting of amino acids, nucleic acids, and sugars, are likely main components of necromass in nature. If a metabolite is detected, a peak height is recorded by the LC-MS instrument, and the area under the curve is calculated. The magnitude of the area under the curve corresponds to the relative abundance of a specific chemical compound. Red colors in this plot represent high abundance of a specific metabolite whereas blue colors represent low abundance. These calculations are also normalized, meaning that the magnitude of abundance is relative to each sample. The dendrogram on top of the figure showcases chemical similarities in metabolite profiles between individual samples.

Table 1. List of microbial isolates that were utilized as artificial necromass and their associated

Necromass Strain	TOC Concentration (ppm)
Pseudomonas helmanticensis strain 28C6	978.45
Paraburkholderia fungorum strain OX1313	1209.95
Microbacterium sp. FQ-57-2	1498.2
Azoarcus evansii strain KB740	1025
Rhodanobacter sp.	554.7

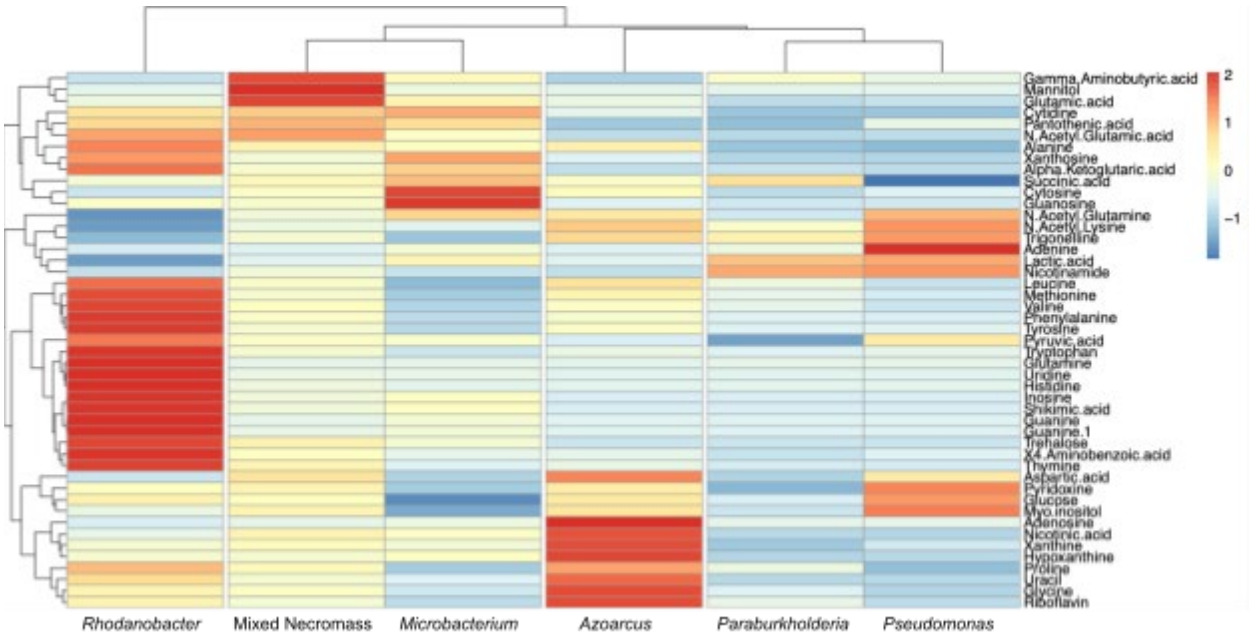

Figure 3. Cluster map of necromass metabolomic composition. Red colors signify high metabolite relative abundance and blue colors signify low metabolite relative abundance.

Microbial Communities Enriched by Necromass

16S Amplicon sequence analysis in QIIME2 and downstream analysis in R produced the relative abundance plots shown in Figure 4. This figure showcases the relative abundances of genera enriched through our experiment. Each box represents a different necromass enrichment condition: 5 individual necromass strains, 1 mixed necromass, and 1 control with no necromass. The plot titled 'Initial' refers to the microbial community composition that was present in the ORR FRC groundwater. The relative abundance of genera enriched throughout our experimentation is represented in percentages on the y-axis. The x-axis represents the four timepoints in which our cultures were sampled, as well as the three replicates conducted. A total of 13 genera were enriched and comprised more than 2% of the community. Out of these 13 genera, 6 are represented in high abundance in each enrichment community: *Bosea*, *Brevundimonas*, *Caulobacter*, *Paenarthrobacter*, *Pseudomonas*, and *Variovorax*. *Pseudomonas* was the most abundant genus enriched in most treatment conditions.

I conducted three alpha diversity tests on my data: Observed, Shannon, and Inverse Simpson. The first two tests assess differences in species richness across our different treatment conditions whereas the Inverse Simpson test focuses on the level of evenness across those groups.

According to my statistical analysis, p-values were higher than the critical value of 0.05 for all three of these tests (Table 2). In addition to alpha diversity, I also assessed beta diversity metrics by using Bray-Curtis Dissimilarity measures. This statistical method helps to determine whether microbial community compositions are significantly different across different treatment groups. My data indicated that there were two experimental conditions that yielded p-values less than the critical value of 0.05. These two groups were the *Rhodanobacter* necromass treatment group and the no necromass control group.

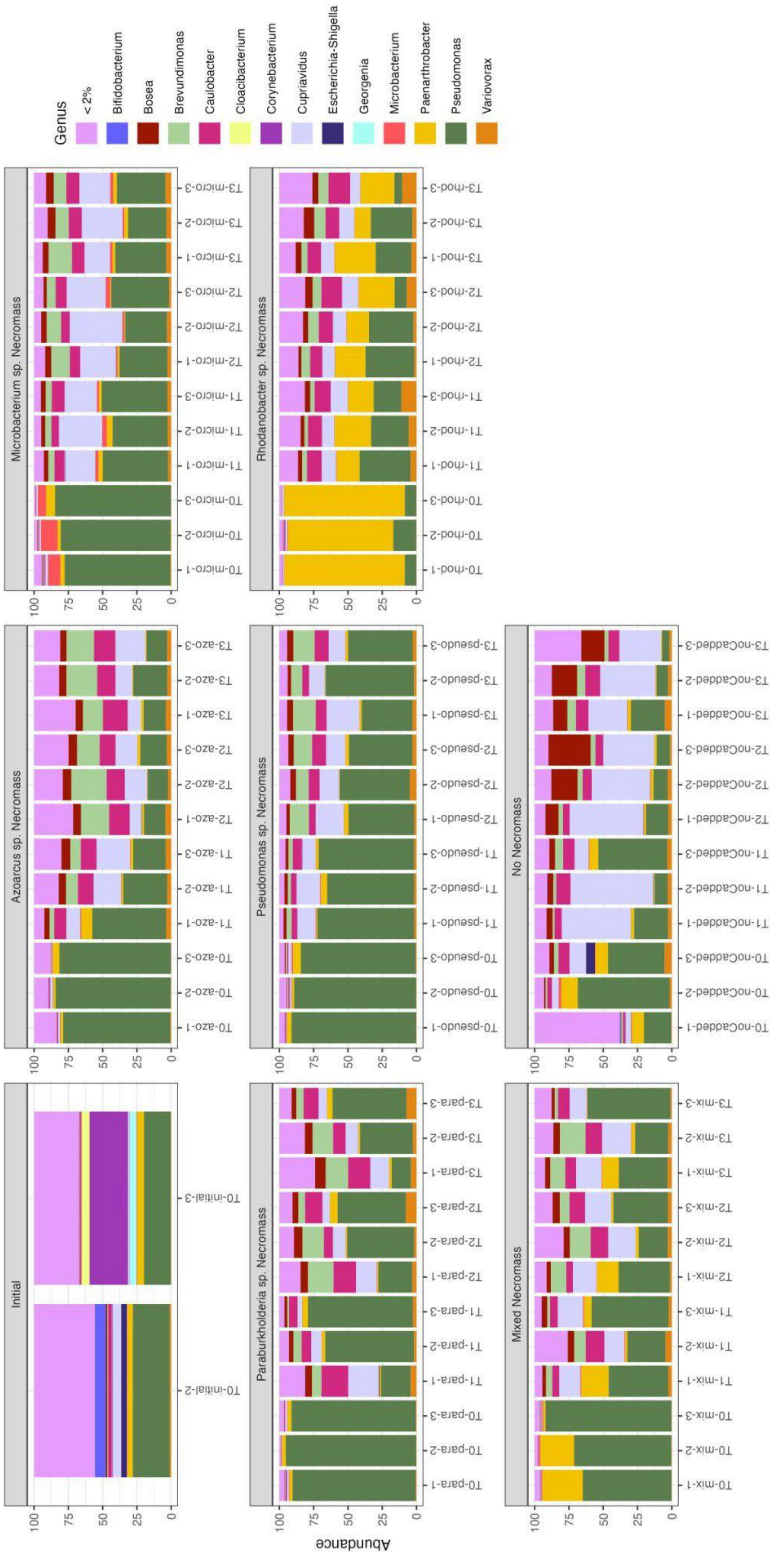

Figure 4: Groundwater microbial community composition over the course of a 3 week incubation period.

Isolates From Groundwater Enrichment in Necromass

The phylogenetic tree in Figure 5 showcases the different genera isolated from my necromass enrichments. Different colors on this tree represent the enrichments in different necromass sources. The bootstraps values on the branches of the tree gives an indication on how reliable a specific grouping is. This number is the likelihood of returning the same branching pattern if the tree were resampled 100 times. I included 7 known bacterial strains as reference points on my tree: *Escherichia coli, Pigmentiphaga kullae, Variovorax guangxiensis, Arthrobacter humicola, Aureimonas phyllosphaerae, Brevundimonas mediterranea, and Bosea robiniae. Escherichia coli* strain U 5/41 was the outgroup in this phylogenetic tree.

Microbacterium sp. necromass, which was utilized in my enrichment experiment, was difficult to grow in basal media and so I decided not to include this as a treatment condition in my isolation efforts. Despite this, I was able to isolate a total of 6 different genera: *Pigmintiphaga*, *Variovorax, Arthrobacter, Aureimonas, Brevundimonas,* and *Bosea.*

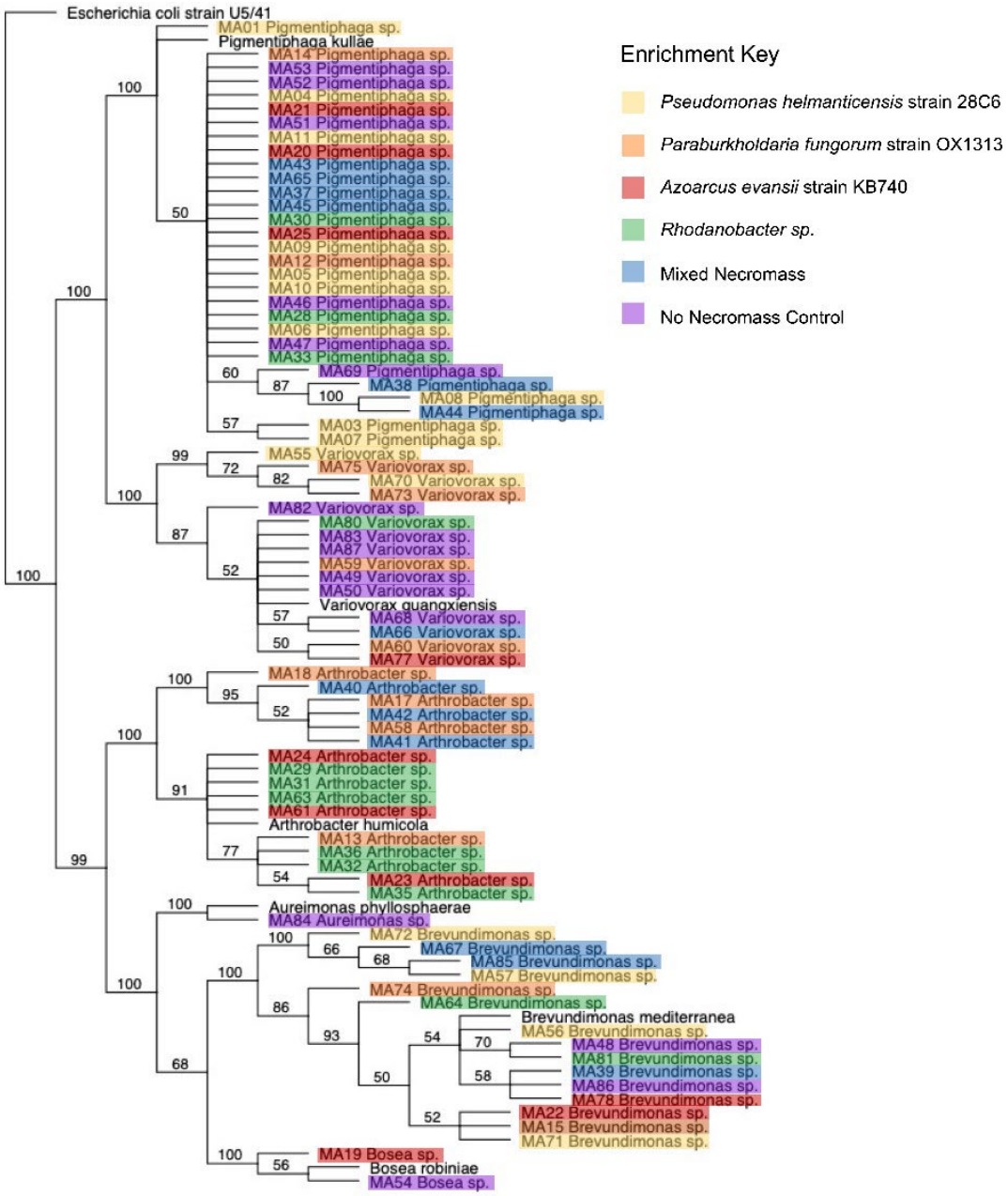

Figure 5: Phylogenetic tree of genera isolated from groundwater enrichments in necromass. Different colors signify different necromass enrichment conditions.

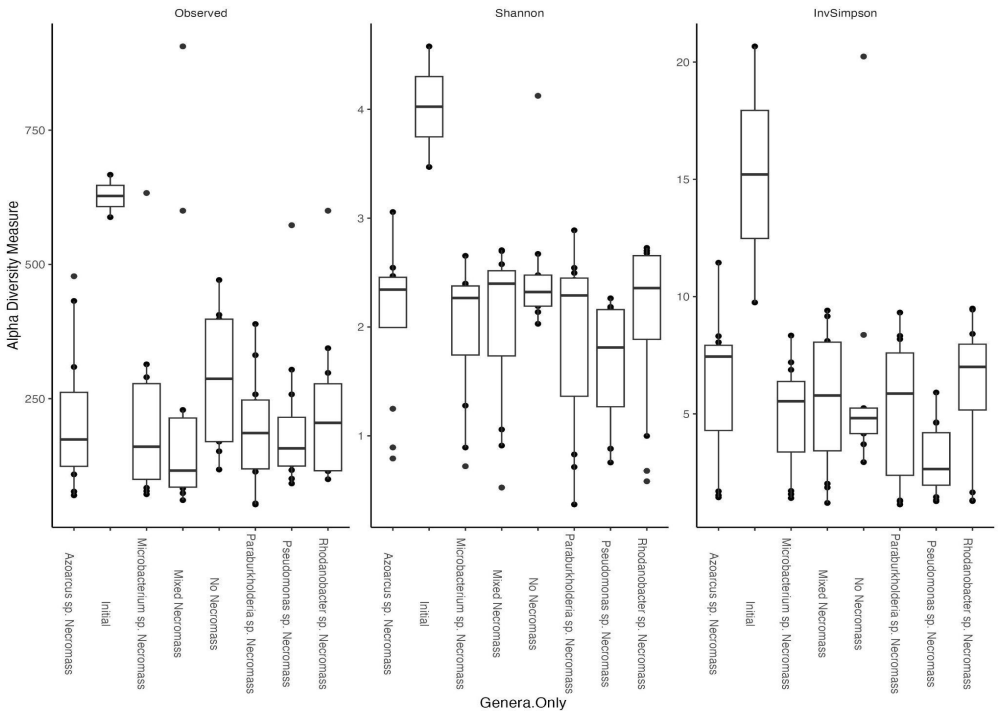

Figure 6: Alpha diversity tests conducted on necromass enrichment data. Observed and Shannon test boxplots visualize species richness in each necromass treatment condition. Inverse Simpson test boxplot visualizes the level of evenness across each condition.

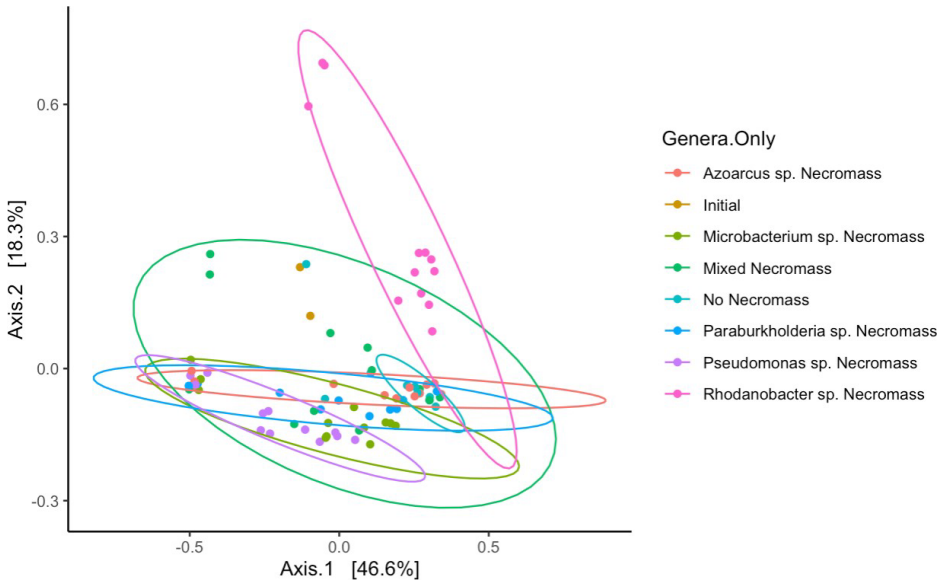

Figure 7: Beta diversity analysis microbial communities enriched in different necromass conditions. Different colors correspond to different necromass treatment groups. Axes reflect non-metric parameters of differences across these different microbial communities.

Table 2: p-values of three alpha diversity tests (Observed, Shannon, and Inverse Simpson) to determine whether different necromass enrichment conditions result in different levels of species richness or evenness.

Observed			Shannon			Inverse Simpson		
group1	group2	p.adj	group1	group2	p.adj	group1	group2	p.adj
Initial	Azoarcus sp. Necromass	0.205128205	Initial	Azoarcus sp. Necromass	0.07692308	Initial	Azoarcus sp. Necromass	0.123076923
Microbacterium sp. Necromass	Azoarcus sp. Necromass	0.932300503	Microbacterium sp. Necromass	Azoarcus sp. Necromass	0.70379512	Microbacterium sp. Necromass	Azoarcus sp. Necromass	0.255375799
Mixed Necromass	Azoarcus sp. Necromass	0.716643197	Mixed Necromass	Azoarcus sp. Necromass	0.89459478	Mixed Necromass	Azoarcus sp. Necromass	0.97227231
No Necromass	Azoarcus sp. Necromass	0.43769605	No Necromass	Azoarcus sp. Necromass	0.89459478	No Necromass	Azoarcus sp. Necromass	0.775308407
Paraburkholderia sp. Necromass	Azoarcus sp. Necromass	0.932300503	Paraburkholderia sp. Necromass	Azoarcus sp. Necromass	0.83963401	Paraburkholderia sp. Necromass	Azoarcus sp. Necromass	0.524728516
Pseudomonas sp. Necromass	Azoarcus sp. Necromass	0.932300503	Pseudomonas sp. Necromass	Azoarcus sp. Necromass	0.07692308	Pseudomonas sp. Necromass	Azoarcus sp. Necromass	0.076923077
Rhodanobacter sp. Necromass	Azoarcus sp. Necromass	0.932300503	Rhodanobacter sp. Necromass	Azoarcus sp. Necromass	0.92025208	Rhodanobacter sp. Necromass	Azoarcus sp. Necromass	0.965517504
Microbacterium sp. Necromass	Initial	0.219866952	Microbacterium sp. Necromass	Initial	0.07692308	Microbacterium sp. Necromass	Initial	0.076923077
Mixed Necromass	Initial	0.335664336	Mixed Necromass	Initial	0.07692308	Mixed Necromass	Initial	0.076923077
No Necromass	Initial	0.219866952	No Necromass	Initial	0.16969697	No Necromass	Initial	0.16969697
Paraburkholderia sp. Necromass	Initial	0.205128205	Paraburkholderia sp. Necromass	Initial	0.07692308	Paraburkholderia sp. Necromass	Initial	0.076923077
Pseudomonas sp. Necromass	Initial	0.205128205	Pseudomonas sp. Necromass	Initial	0.07692308	Pseudomonas sp. Necromass	Initial	0.076923077
Rhodanobacter sp. Necromass	Initial	0.219866952	Rhodanobacter sp. Necromass	Initial	0.07692308	Rhodanobacter sp. Necromass	Initial	0.076923077
Mixed Necromass	Microbacterium sp. Necromass	0.932300503	Mixed Necromass	Microbacterium sp. Necromass	0.69523556	Mixed Necromass	Microbacterium sp. Necromass	0.703795117
No Necromass	Microbacterium sp. Necromass	0.267263634	No Necromass	Microbacterium sp. Necromass	0.49381826	No Necromass	Microbacterium sp. Necromass	0.97227231
Paraburkholderia sp. Necromass	Microbacterium sp. Necromass	0.932300503	Paraburkholderia sp. Necromass	Microbacterium sp. Necromass	0.90766953	Paraburkholderia sp. Necromass	Microbacterium sp. Necromass	0.965517504
Pseudomonas sp. Necromass	Microbacterium sp. Necromass	0.932300503	Pseudomonas sp. Necromass	Microbacterium sp. Necromass	0.14522091	Pseudomonas sp. Necromass	Microbacterium sp. Necromass	0.120465765
Rhodanobacter sp. Necromass	Microbacterium sp. Necromass	0.717509644	Rhodanobacter sp. Necromass	Microbacterium sp. Necromass	0.69523556	Rhodanobacter sp. Necromass	Microbacterium sp. Necromass	0.267246515
No Necromass	Mixed Necromass	0.219866952	No Necromass	Mixed Necromass	0.8935634	No Necromass	Mixed Necromass	0.97227231
Paraburkholderia sp. Necromass	Mixed Necromass	0.799124015	Paraburkholderia sp. Necromass	Mixed Necromass	0.70379512	Paraburkholderia sp. Necromass	Mixed Necromass	0.965517504
Pseudomonas sp. Necromass	Mixed Necromass	0.663612055	Pseudomonas sp. Necromass	Mixed Necromass	0.16969697	Pseudomonas sp. Necromass	Mixed Necromass	0.151854338
Rhodanobacter sp. Necromass	Mixed Necromass	0.395730633	Rhodanobacter sp. Necromass	Mixed Necromass	0.89459478	Rhodanobacter sp. Necromass	Mixed Necromass	0.950046768
Paraburkholderia sp. Necromass	No Necromass	0.267263634	Paraburkholderia sp. Necromass	No Necromass	0.69523556	Paraburkholderia sp. Necromass	No Necromass	0.965517504
Pseudomonas sp. Necromass	No Necromass	0.267263634	Pseudomonas sp. Necromass	No Necromass	0.01848059	Pseudomonas sp. Necromass	No Necromass	0.076923077
Rhodanobacter sp. Necromass	No Necromass	0.386561256	Rhodanobacter sp. Necromass	No Necromass	0.97227231	Rhodanobacter sp. Necromass	No Necromass	0.656611362
Pseudomonas sp. Necromass	Paraburkholderia sp. Necromass	0.932300503	Pseudomonas sp. Necromass	Paraburkholderia sp. Necromass	0.42604825	Pseudomonas sp. Necromass	Paraburkholderia sp. Necromass	0.255375799
Rhodanobacter sp. Necromass	Paraburkholderia sp. Necromass	0.932300503	Rhodanobacter sp. Necromass	Paraburkholderia sp. Necromass	0.77163403	Rhodanobacter sp. Necromass	Paraburkholderia sp. Necromass	0.524728516
Rhodanobacter sp. Necromass	Pseudomonas sp. Necromass	0.932300503	Rhodanobacter sp. Necromass	Pseudomonas sp. Necromass	0.12046577	Rhodanobacter sp. Necromass	Pseudomonas sp. Necromass	0.076923077

Table 3: p-values of Bray-Curtis Dissimilarity test to determine whether different necromass enrichment conditions result in different microbial community compositions

Group 1	Group 2	p	p.adj
Initial	Pseudomonas sp. Necromass	0.012	0.02584615
Initial	Microbacterium sp. Necromass	0.016	0.02986667
Initial	Azoarcus sp. Necromass	0.041	0.0574
Initial	Rhodanobacter sp. Necromass	0.015	0.02986667
Initial	Mixed Necromass	0.018	0.0315
Initial	Paraburkholderia sp. Necromass	0.012	0.02584615
Initial	No Necromass	0.026	0.04044444
Pseudomonas sp. Necromass	Microbacterium sp. Necromass	0.053	0.07066667
Pseudomonas sp. Necromass	Azoarcus sp. Necromass	0.021	0.03458824
Pseudomonas sp. Necromass	Rhodanobacter sp. Necromass	0.001	0.0035
Pseudomonas sp. Necromass	Mixed Necromass	0.083	0.10563636
Pseudomonas sp. Necromass	Paraburkholderia sp. Necromass	0.096	0.11686957
Pseudomonas sp. Necromass	No Necromass	0.001	0.0035
Microbacterium sp. Necromass	Azoarcus sp. Necromass	0.034	0.05010526
Microbacterium sp. Necromass	Rhodanobacter sp. Necromass	0.001	0.0035
Microbacterium sp. Necromass	Mixed Necromass	0.171	0.18415385
Microbacterium sp. Necromass	Paraburkholderia sp. Necromass	0.11	0.12833333
Microbacterium sp. Necromass	No Necromass	0.004	0.01018182
Azoarcus sp. Necromass	Rhodanobacter sp. Necromass	0.001	0.0035
Azoarcus sp. Necromass	Mixed Necromass	0.156	0.17472
Azoarcus sp. Necromass	Paraburkholderia sp. Necromass	0.227	0.23540741
Azoarcus sp. Necromass	No Necromass	0.001	0.0035
Rhodanobacter sp. Necromass	Mixed Necromass	0.002	0.00622222
Rhodanobacter sp. Necromass	Paraburkholderia sp. Necromass	0.001	0.0035
Rhodanobacter sp. Necromass	No Necromass	0.001	0.0035
Mixed Necromass	Paraburkholderia sp. Necromass	0.411	0.411
Mixed Necromass	No Necromass	0.001	0.0035
Paraburkholderia sp. Necromass	No Necromass	0.004	0.01018182

DISCUSSION

Necromass (ie. non-living microbial biomass) is an important component of soil organic matter, which plays an essential role in carbon cycling dynamics. The goal of my experiment is to investigate the dynamics of groundwater microbial necrophagy by examining composition of artificial necromass, using it as a substrate to enrich and isolate groundwater microbial communities. By learning more about which microbes that actively consume necromass as a main carbon source in subsurface ecosystems, we can better understand carbon turnover rates and determine the extent at which the subsurface acts as a carbon sink.

Different Strains of Necromass Yield Different Metabolomic Compositions

My metabolomic analysis conducted on the five necromass strains revealed that necromass composition does vary depending on the species used (Figure 3). According to this mapping, *Paraburkholderia* and *Pseudomonas* necromass strains have chemical compositions that are most similar to each other when compared to any other necromass strain. Their similarities are attributed to having similar relative abundances of N-acetyl lysine, trigonelline, lactic acid, and nicotinamide. Other necromass strains appear to differ to a greater extent, with *Rhodanobacter* necromass having a chemical composition that differs the most from all other strains. The degree of difference in *Rhodanobacter*'s chemical composition is attributed to its high abundance in leucine, methionine, valine, phenylalanine, tyrosine, pyruvic acid, tryptophan, glutamine, uridine, histidine, inosine, shikimic acid, guanine, and trehalose. While these compounds are abundant in *Rhodanobacter* necromass, they are of low abundance or even lacking in other necromass strains. The metabolomic composition of *Azoarcus* necromass is also unique because it was found to have high abundance of adenosine, nicotinic acid, xanthine, hypoxanthine, pyroline, uracil, glycine, and riboflavin. Similarly with *Rhodanobacter* necromass, where the chemical compounds are abundant in *Azoarcus* necromass, they tend to be scarce in other necromass strains.

The overproduction of metabolites is influenced by the development phases of a certain microorganism. Intracellular inducers, effectors, inhibitors, and signal molecules influence microbial metabolism in different ways depending on the development phase that a microbe is in (Sanchez and Demain, 2008). Knowing this, a possible reason why the bacterial strains that I

utilized as necromass differed in metabolite composition could be because I harvested these strains and turned them into necromass at different times. In future experimentation, it would be beneficial to generate necromass from different strains along the same timeline. If this does not prove to be the main factor in shaping metabolomics, then it is likely that the development phases of different microbes are structured differently. An important point to note is that all of the bacterial strains utilized were isolated from ORR FRC, a field site known to be hazardous and radioactive in consequence of it being used as a waste disposal unit (Watson et al. 2004). Because microbial metabolism is affected by factors like pH and total phosphorus, it is likely that the bacterial strains studied in my experiment have been significantly altered by living in such harsh conditions (Cao et al. 2016). This preliminary metabolomic analysis was done to get a general idea of necromass chemical composition, however, further work should be conducted to get a better understanding about these subsurface processes. It would be beneficial to conduct multiple trials of this study and incorporate more microbial strains to reflect the in situ microbiological diversity and complexity.

Influence of Necromass Metabolomic Composition on Groundwater Microbial Communities

I investigated differences in microbial community compositions across different treatment groups by conducting alpha and beta diversity analyses. Alpha diversity metrics examine the level of inherent diversity present within a specific community (Figure 6) (Walters et al. 2020). My finding of p-values greater than 0.05 (Table 2) indicates that there is no significant difference in species richness or evenness between any of my treatment groups. In other words, introducing different types of necromass to a groundwater microbial community does not have an impact on the number of species or their composition within that community. This is likely due to the fact that the most abundant species are all capable of utilizing necromass as a carbon source.

Beta diversity metrics look at how different the microbial community compositions of one treatment group is different from the rest (Figure 7) (Walters et al. 2020). My data indicated that my *Rhodanobacter* necromass treatment group and my No Necromass control group resulted in microbial committees that differed significantly from any other enrichment condition. These results imply that microbial community compositions are significantly influenced by the introduction of necromass; this aligns with previous studies revealing that microbial diversity increases with enrichments in complex carbon sources like necromass (Wu et al. 2020).

Additionally, the strain of necromass introduced also has a significant impact on the resulting microbial community (Dong et al. 2021). In my pilot study on necromass metabolomics, it was found that *Rhodanobacter* necromass had the most unique chemical composition relative to any other necromass strain studied in my experiment. This finding could be a key factor in why the microbial community composition of *Rhodanobacter* necromass enrichments differed significantly from any of other necromass enrichment conditions.

Isolating Groundwater Strains in Necromass

Glycerol stocks from the last sampled timepoint of my groundwater enrichment experiment were the main focus of my isolation efforts. I was interested in identifying the microbial strains present at the end of our incubation period because these are likely to be the ones that actively consume necromass in nature. Out of the 7 most abundant genera in my enrichments in necromass (*Bosea*, *Brevundimonas*, *Caulobacter*, *Paenarthrobacter*, *Pseudomonas*, and *Variovorax)*, I was only able to isolate 3 of them (*Bosea, Brevundimonas, and Variovorax*). This could be attributed to the fact that microbes interact differently on solid media versus in liquid media. Alternatively, another cause for the lack of diversity in my isolates could be that my groundwater sample was too concentrated. I initially started isolations with undiluted groundwater but once I observed that many plates were full of identical colony types, I decided to try out 10^{-1} and 10^{-2} dilutions. These resulted in more diverse colony types but I suspect that if I conducted isolations with even more diluted groundwater, I would be able to isolate other genera that were enriched in necromass.

An important finding is that many isolates were able to grow in my no necromass control sample. Although there is no way to determine with certainty what these microbes were consuming, it is likely that they were utilizing dead members of their own community as a carbon source. Whether these microbes are consuming my artificial necromass media or the remains of cells from the groundwater inoculum that grew up and died during incubation, these communities are consuming a form of dead microbial biomass.

Conclusions and Future Applications

Necromass plays an important role as a carbon source in subsurface ecosystems.

According to my data, the introduction of necromass to a groundwater microbial community significantly influences the resulting microbial composition. Results from my necromass metabolomics analysis indicate that necromass chemical composition differs with the species of cell lysate used to produce it. This finding was used to explain why in my *Rhodanobacter* necromass treatment group yielded a microbial community composition significantly different from any other treatment condition. This finding may help us in understanding the different ways that microbes are able to utilize carbon in the subsurface.

Because my metabolomics data was part of a preliminary study, it would be beneficial to conduct an in-depth investigation of the chemical composition of different necromass strains and explore this data statistically. This would include running multiple trials of metabolomics analysis and incorporating many other strains of bacteria to statistically infer the extent at which necromass chemical composition varies. Additionally, stable isotope probing techniques could be integrated in future incubations to target microbes that are actively consuming artificial necromass and not dead cells from the groundwater matrix. It would also be of value to expand my groundwater enrichment experiments to include other cell lysates to reflect the complexity and biodiversity of the subsurface microbiome. Although my mixed necromass enrichment condition was intended to serve as a more accurate representative of what necromass may look like in groundwater ecosystems, in reality, necromass in nature is much more complex. Since *Rhodanobacter* necromass was the only type of necromass in my study to yield significantly different microbial community compositions, exploring this phenomenon with other chemically unique necromass strains would help us to gain insight into how carbon is utilized in these groundwater microbial communities. By understanding the dynamics of necromass utilization and its role in subsurface ecosystems, we can learn more about carbon cycling dynamics and determine the extent at which the subsurface acts as a carbon sink.

ACKNOWLEDGEMENTS

I would like to thank my friends and colleagues at the Chakraborty Lab in Lawrence Berkeley National Laboratory for enthusiastically guiding me through my senior thesis. I am especially grateful for my mentor, Dr. Brandon Enalls, a postdoctoral scholar with this group, and my principal investigator, Dr. Romy Chakraborty, for their patience and kindness as we navigated this project together. I am also very appreciative of the environmental science senior thesis teaching team, namely Patina Mendez, Danielle Perryman, and Robin Lopez, for their words of

encouragement and their friendship throughout these past 2 years. Lastly, I would like to thank my family and friends for always believing in me, motivating me, and reminding me that everything will fall into place eventually.

REFERENCES

Adingo, S., J.-R. Yu, L. Xuelu, X. Li, S. Jing, and Z. Xiaong. 2021. Variation of soil microbial carbon use efficiency (CUE) and its Influence mechanism in the context of global environmental change: a review. PeerJ 9:e12131.

Basile-Doelsch, I., J. Balesdent, and S. Pellerin. 2020. Reviews and syntheses: The mechanisms underlying carbon storage in soil. Biogeosciences 17:5223–5242.

Bolyen, E., J. R. Rideout, M. R. Dillon, N. A. Bokulich, C. C. Abnet, G. A. Al-Ghalith, H. Alexander, E. J. Alm, M. Arumugam, F. Asnicar, Y. Bai, J. E. Bisanz, K. Bittinger, A. Brejnrod, C. J. Brislawn, C. T. Brown, B. J. Callahan, A. M. Caraballo-Rodríguez, J. Chase, E. K. Cope, R. Da Silva, C. Diener, P. C. Dorrestein, G. M. Douglas, D. M. Durall,

C. Duvallet, C. F. Edwardson, M. Ernst, M. Estaki, J. Fouquier, J. M. Gauglitz, S. M. Gibbons, D. L. Gibson, A. Gonzalez, K. Gorlick, J. Guo, B. Hillmann, S. Holmes, H. Holste, C. Huttenhower, G. A. Huttley, S. Janssen, A. K. Jarmusch, L. Jiang, B. D. Kaehler,

K. B. Kang, C. R. Keefe, P. Keim, S. T. Kelley, D. Knights, I. Koester, T. Kosciolek, J. Kreps, M. G. I. Langille, J. Lee, R. Ley, Y.-X. Liu, E. Loftfield, C. Lozupone, M. Maher, C. Marotz, B. D. Martin, D. McDonald, L. J. McIver, A. V. Melnik, J. L. Metcalf, S. C. Morgan, J. T. Morton, A. T. Naimey, J. A. Navas-Molina, L. F. Nothias, S. B. Orchanian, T. Pearson, S. L. Peoples, D. Petras, M. L. Preuss, E. Pruesse, L. B. Rasmussen, A. Rivers, M.

S. Robeson, P. Rosenthal, N. Segata, M. Shaffer, A. Shiffer, R. Sinha, S. J. Song, J. R. Spear, A. D. Swafford, L. R. Thompson, P. J. Torres, P. Trinh, A. Tripathi, P. J. Turnbaugh,

S. Ul-Hasan, J. J. J. van der Hooft, F. Vargas, Y. Vázquez-Baeza, E. Vogtmann, M. von Hippel, W. Walters, Y. Wan, M. Wang, J. Warren, K. C. Weber, C. H. D. Williamson, A. D. Willis, Z. Z. Xu, J. R. Zaneveld, Y. Zhang, Q. Zhu, R. Knight, and J. G. Caporaso. 2019.

Reproducible, interactive, scalable and extensible microbiome data science using QIIME 2. Nature Biotechnology 37:852–857.

Bradford, M. A., W. R. Wieder, G. B. Bonan, N. Fierer, P. A. Raymond, and T. W. Crowther. 2016. Managing uncertainty in soil carbon feedbacks to climate change. Nature Climate Change 6:751–758.

Buckeridge, K. M., C. Creamer, and J. Whitaker. 2022. Deconstructing the microbial necromass continuum to inform soil carbon sequestration. Functional Ecology:1365-2435.14014.

Cao, H., R. Chen, L. Wang, L. Jiang, F. Yang, S. Zheng, G. Wang, and X. Lin. 2016. Soil pH, total phosphorus, climate and distance are the major factors influencing microbial activity

at a regional spatial scale. Scientific Reports 6:25815.

Dong, W., A. Song, H. Yin, X. Liu, J. Li, and F. Fan. 2021. Decomposition of Microbial Necromass Is Divergent at the Individual Taxonomic Level in Soil. Frontiers in Microbiology 12:679793.

Eswaran, H., E. Van Den Berg, and P. Reich. 1993. Organic Carbon in Soils of the World. Soil Science Society of America Journal 57:192–194.

Jackson, R. B., K. Lajtha, S. E. Crow, G. Hugelius, M. G. Kramer, and G. Piñeiro. 2017. The Ecology of Soil Carbon: Pools, Vulnerabilities, and Biotic and Abiotic Controls. Annual Review of Ecology, Evolution, and Systematics 48:419–445.

Kassambara, A. and Mundt, F. (2020) Factoextra: Extract and Visualize the Results of Multivariate Data Analyses. R Package Version 1.0.7.

https://CRAN.R-project.org/package=factoextra

Kästner, M., A. Miltner, S. Thiele-Bruhn, and C. Liang. 2021. Microbial Necromass in Soils—Linking Microbes to Soil Processes and Carbon Turnover. Frontiers in Environmental Science 9:756378.

Kolde, Raivo. "Pheatmap: pretty heatmaps." R package version 1.2 (2012): 726. https://CRAN.R-project.org/package=pheatmap

Liang, C., W. Amelung, J. Lehmann, and M. Kästner. 2019. Quantitative assessment of microbial necromass contribution to soil organic matter. Global Change Biology 25:3578–3590.

Love, M. I., W. Huber, and S. Anders. 2014. Moderated estimation of fold change and dispersion for RNA-seq data with DESeq2. Genome Biology 15:550.

Maechler M, Rousseeuw P, Struyf A, Hubert M, Hornik K (2022). cluster: Cluster Analysis Basics and Extensions. R package version 2.1.4 — For new features, see the 'Changelog' file (in the package source), https://CRAN.R-project.org/package=cluster.

Martins, S. J., S. J. Taerum, L. Triplett, J. B. Emerson, I. Zasada, B. F. de Toledo, J. Kovac, K. Martin, and C. T. Bull. 2022. Predators of Soil Bacteria in Plant and Human Health.

Phytobiomes Journal:PBIOMES-11-21-0073-RVW.

McMurdie and Holmes (2014) Shiny-phyloseq: Web Application for Interactive Microbiome Analysis with Provenance Tracking. Bioinformatics (Oxford, England) 31(2), 282–283.

Oksanen J, Simpson G, Blanchet F, Kindt R, Legendre P, Minchin P, O'Hara R, Solymos P, Stevens M, Szoecs E, Wagner H, Barbour M, Bedward M, Bolker B, Borcard D, Carvalho G, Chirico M, De Caceres M, Durand S, Evangelista H, FitzJohn R, Friendly M, Furneaux B, Hannigan G, Hill M, Lahti L, McGlinn D, Ouellette M, Ribeiro Cunha E, Smith T, Stier A, Ter Braak C, Weedon J (2022). _vegan: Community Ecology Package_. R

package version 2.6-4, https://CRAN.R-project.org/package=vegan.

Sanchez, S., and A. L. Demain. 2008. Metabolic regulation and overproduction of primary metabolites: Metabolic regulation and overproduction of primary metabolites. Microbial Biotechnology 1:283–319.

Sokol, N. W., J. Sanderman, and M. A. Bradford. 2019. Pathways of mineral-associated soil organic matter formation: Integrating the role of plant carbon source, chemistry, and point of entry. Global Change Biology 25:12–24.

Walters, K. E., and J. B. H. Martiny. 2020. Alpha-, beta-, and gamma-diversity of bacteria varies across habitats. PLOS ONE 15:e0233872.

Watson, D. B., J. E. Kostka, M. W. Fields, and P. M. Jardine. 1995. The Oak Ridge Field Research Center Conceptual Model.

Wickham H (2016). ggplot2: Elegant Graphics for Data Analysis. Springer-Verlag New York.

ISBN 978-3-319-24277-4, https://ggplot2.tidyverse.org.

Wickham, H., M. Averick, J. Bryan, W. Chang, L. McGowan, R. François, G. Grolemund, A. Hayes, L. Henry, J. Hester, M. Kuhn, T. Pedersen, E. Miller, S. Bache, K. Müller, J. Ooms,

D. Robinson, D. Seidel, V. Spinu, K. Takahashi, D. Vaughan, C. Wilke, K. Woo, and H. Yutani. 2019. Welcome to the Tidyverse. Journal of Open Source Software 4:1686.

Wu, X., S. Spencer, S. Gushgari-Doyle, M. O. Yee, J. Voriskova, Y. Li, E. J. Alm, and R. Chakraborty. 2020. Culturing of "Unculturable" Subsurface Microbes: Natural Organic Carbon Source Fuels the Growth of Diverse and Distinct Bacteria From Groundwater. Frontiers in Microbiology 11:610001.